Key Engineering Materials
ISSN: 1662-9795, Vol. 1047, pp 259-265

Submitted: 2026-01-26
Revised: 2026-02-16
Accepted: 2026-02-25
Online: 2026-04-13

Influence of Local Laser Power Distribution and Build-Plate Temperature on Porosity and Microstructure in Laser Powder Bed Fusion (LPBF)

Chukwuemeka Okolo[1,a*], Sebastian Härtel[1,b]

[1]Chair of Hybrid Manufacturing (FHF), Brandenburg University of Technology, 03046 Cottbus, Germany

[a*]Okolo@b-tu.de, [b]haertel@b-tu.de

Keywords: laser powder bed fusion (LPBF), porosity, build-plate temperature.

Abstract. Laser powder bed fusion (LPBF) parts are commonly fabricated using nominally uniform process parameters; however, local variations in thermal boundary conditions can significantly influence part quality. In this study, the spatial distribution of build-plate temperature during LPBF of Inconel 718 was experimentally characterized using a thermocouple grid, and its influence on porosity, microstructure and hardness was investigated. Despite a nominal build-plate set temperature of 180 °C, measured temperatures ranged from approximately 101 °C to 120 °C and exhibited a pronounced radial gradient from the center toward the edges of the build-plate. Cubic samples fabricated at locations corresponding to the highest and lowest local temperatures showed distinct microstructural differences, with higher temperatures promoting slightly coarser cellular–dendritic morphologies and lower hardness values. Although bulk volumetric porosity showed identical values for both locations (≈0.01 vol.%), the pore populations differed: the hotter location contained fewer but locally larger voids while the cooler location exhibited a higher number density of smaller pores, as shown by equivalent-diameter histograms and cumulative distributions. Samples produced at cooler locations exhibited finer microstructures and higher hardness. These results demonstrate that spatial non-uniformity in build-plate temperature can lead to local variations in microstructure and mechanical properties within a single LPBF build, highlighting the importance of characterizing local thermal conditions when establishing reliable process-structure property relationships.

Introduction

Laser powder bed fusion (LPBF) is a leading additive manufacturing method for producing complex, high-performance metal components because it enables near-net-shape fabrication with high geometrical freedom and rapid production rates [1], [2]. The quality of LPBF parts is dependent on local thermal conditions and the delivered laser energy, and small variations in these inputs can result in large differences in pore formation, solidification morphology, and resulting mechanical properties [3]. Standard experimental studies commonly report nominal process parameters such as laser power, scan speed, hatch spacing and a global build-plate preheat temperature, but these studies frequently assume that energy delivery and build-plate temperature are spatially uniform across the build-plate [4], [5], [6]. In real production environments, the build-plate temperature often shows substantial spatial variation caused by heater zoning, non-uniform contact to fixtures, thermal losses at plate edges, and localized differences in gas flow or convection [7]. Such build-plate temperature non-uniformity modifies the local thermal boundary condition and therefore changes heat extraction during melting and solidification at the molten track [8]. For nickel-base superalloys like Inconel 718, changes in cooling rate, driven by build-plate temperature shifts can alter cell or dendrite spacing and the kinetics of precipitation, and these microstructural changes influence hardness and local mechanical response [9]. Because the thermal boundary condition controls the solidification rate, spatial differences in build-plate temperature can change whether adjacent tracks are fully remelted or whether lack-of-fusion defects form, even when laser settings are unchanged [10].

Local deviations in delivered laser energy at the work plane, for example due to beam profile imperfections, variable spot size, or optics misalignment, also change the local melt-pool energy density and can move a location between conduction, lack-of-fusion, or keyhole regimes [11]. Melt-pool fluid flow and vapor depression behavior respond to both instantaneous energy input and the substrate boundary condition, so the joint state of local laser energy and build-plate temperature determines the instantaneous thermal history of a powder layer [12].

Despite the separate acknowledgement of beam quality and preheat importance, few studies have systematically mapped both local laser-energy distribution and plate thermal fields across the build area and then directly correlated those spatial maps with position-resolved porosity and microstructure. Prior work has established process maps for defect regimes and demonstrated the sensitivity of melt-pool geometry to local specific energy, but most investigations assume spatial uniformity or report only single-point measurements [11]. Similarly, preheat studies typically report mean platen temperature effects on porosity or microstructure [7], [8] without quantifying intra-plate gradients or their interaction with local beam heterogeneity. This leaves a critical gap: how do spatial overlaps between low (or high) local specific energy and cold (or hot) platen spots jointly influence the formation, type and connectivity of pores, and the resultant microstructural heterogeneity within a single build.

The present study investigates the influence of build-plate temperature on porosity, microstructure and hardness by measuring build-plate temperature with a thermocouple grid, and placing test samples at mapped locations so that each sample is associated with a documented local thermal history.

Materials and Methods

In this study, the spatial distribution of laser energy delivered across the build platform was not measured due to time constraints and the unavailability of a mobile power-measurement instrument for short-term irradiation with solid-state lasers.

To measure the temperature of the build-plate, holes of diameter 1.5mm, and depth of 4mm were drilled on the plate in a grid arrangement as shown in Figure 1 . Thermocouples were placed in these holes to measure the temperature at different locations on the platform. The build-plate was heated up to 180°C and maintained for two hours before taking temperature measurement. The recorded temperatures were interpolated and plotted as a colour-coded grid. Geometries were printed on specified locations on the build-plate and characterized through microscopic analysis for grain morphology and texture. Hardness testing was carried out on these samples for mechanical properties. Cubic specimens (10 × 10 × 14 mm) were fabricated at these locations. Fabrication was performed on an SLM280 system operating in an argon atmosphere. The x-y surface areas were ground (P220-P2500) and polished using diamond suspension of 6µm, 3µm, and 1µm successively. The morphology of the microstructure was observed using a Phenom XL Generation 2 scanning electron microscope (SEM) (FEI Deutschland GmbH / Thermofisher Scientific). The porosity was determined using X-ray micro-computed tomography (µCT) on a TESCAN CoreTOM system (Tescan, Brno, Czech Republic) with a voxel size of 10 µm. The sizes of three-dimensional pores, expressed as equivalent sphere diameters, were determined using Volume Graphics VGSTUDIO MAX 2021 software. HV0.5 Vickers microhardness tests were carried out using the ZwickRoell DuraScan 70 hardness testing machine. Indentations were positioned at the center of the polished cross-sections, with a distance of 1.5 mm between each one.

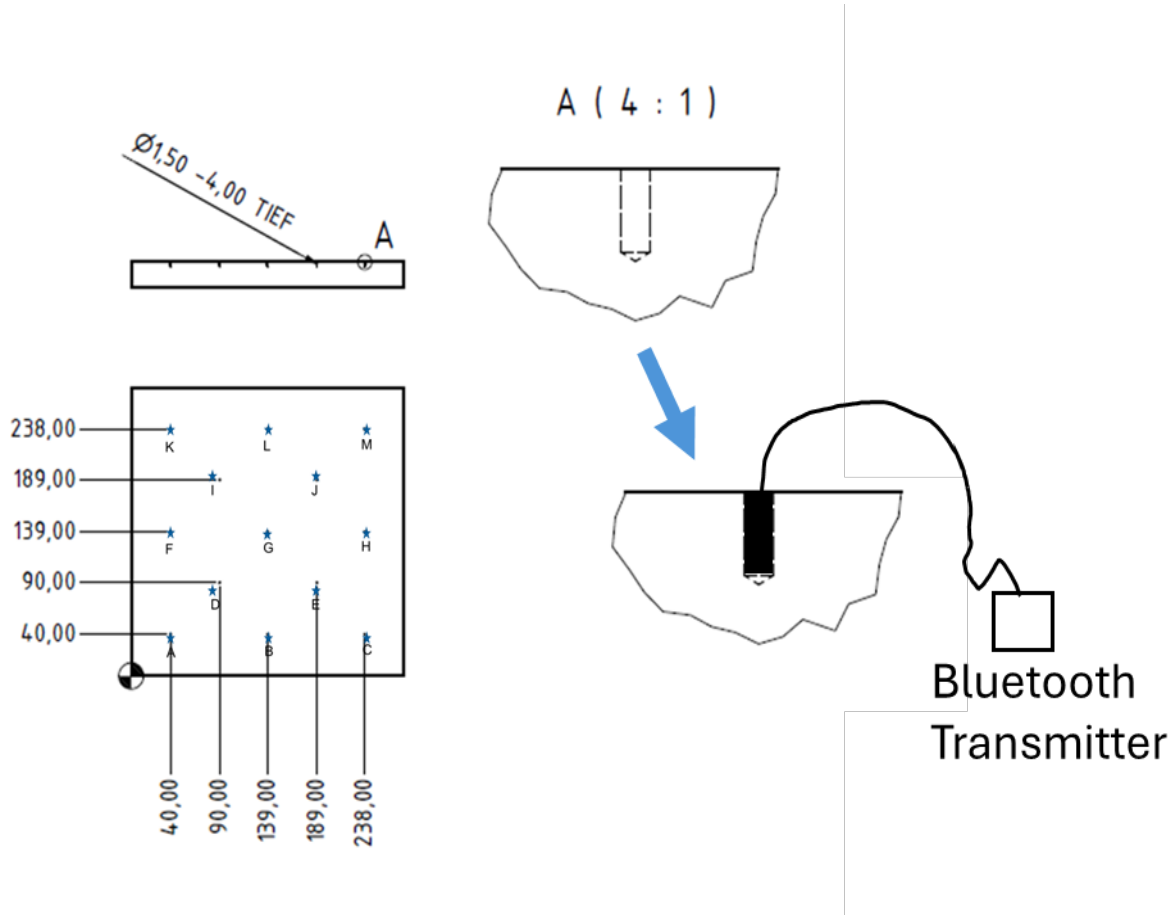

Fig. 1. Placement of thermocouple on the build platform to measure spatial build-plate temperature distribution.

Results and Discussion

Build-plate temperature

Figure 2 shows the temperature map obtained for the In718 build-plate. Although the nominal set build-plate temperature for In718 was 180°C, the measured temperatures were significantly lower and exhibited pronounced spatial variations across the plate. Measured temperatures ranged from approximately 101°C to 120°C, indicating a maximum temperature difference of 19 °C across the build-plate. The highest temperatures were consistently observed in the central region of the plate (position G), while lower temperatures were recorded toward the edges and corners (positions A, K, and M). This temperature gradient reflects non-uniform heat transfer conditions, likely governed by the build-plate heating mechanism, thermal contact resistance, and enhanced heat losses at the plate boundaries. The observed temperature field demonstrates a radially decreasing trend from the center toward the edges. Furthermore, the measured temperatures show a significant deviation from the nominal set build-plate temperature, indicating that the programmed value does not directly reflect the local thermal state experienced by the material during fabrication. This highlights the importance of experimentally characterizing local build-plate temperatures when evaluating spatial variations in microstructure and mechanical properties.

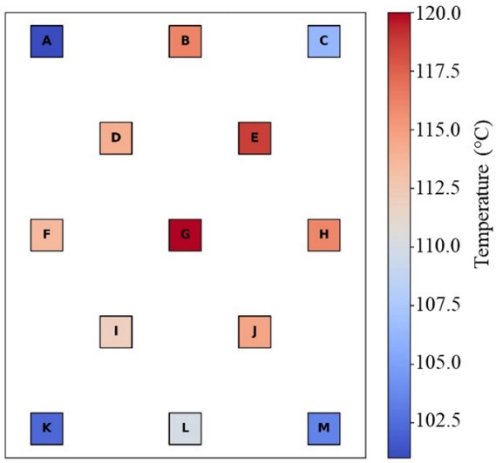

Fig. 2. Spatial distribution of the build-plate temperature across the build surface.

Porosity and relative density

Volumetric porosity quantified by µCT showed approximately the same value of 0.01%. for both positions on the build-plate. Despite equal global porosity, the pore populations differ markedly in morphology and size distribution. The sample at position G (hotter location) contains fewer pores but a small population of larger voids concentrated locally within the scanned volume. By contrast, the sample at position K (colder location) contains a greater number density of smaller pores distributed more uniformly throughout the volume. These contrasting morphologies are reflected in the equivalent-diameter histograms and cumulative curves shown in Figure 3. The distribution of position G is dominated by a narrow peak with a tail of large pores, whereas Position K shows a broader distribution with a heavier count of small features. The observation of equal total porosity but different defect-size architectures indicates that local build-plate temperature controls the defect formation pathway rather than only changing net void volume.

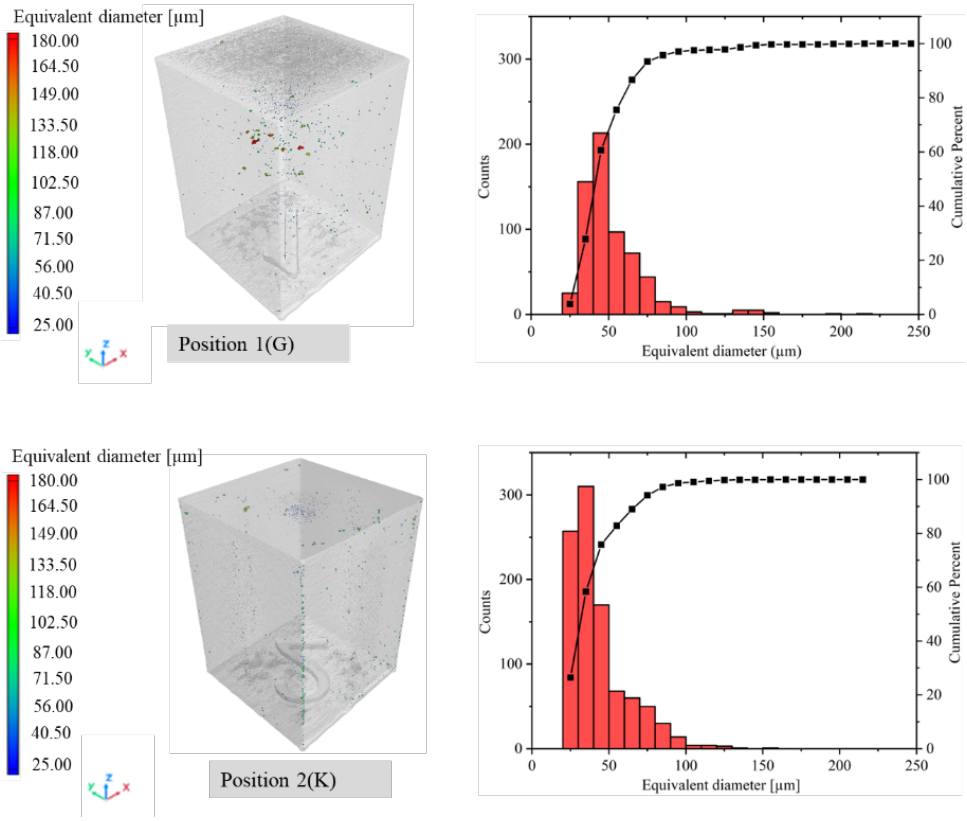

Fig. 3. X-ray micro-computed tomography image and histogram of the pore size distribution.

Microscopy

Figure 4 shows the SEM micrographs of the printed coupons at the highest and lowest build-plate temperature locations. Both samples exhibit the characteristic LPBF microstructure composed of melt-pool related features and a fine cellular-dendritic substructure. However, differences are observed between the two locations. The sample fabricated at position G, corresponding to the higher local build-plate temperature, shows a slightly coarser cellular morphology, suggesting enhanced thermal exposure and reduced cooling rates during solidification. In contrast, the microstructure at position K, which experienced a lower build-plate temperature, appears finer with more pronounced cellular contrast, indicative of higher cooling rates and increased thermal gradients. These microstructural differences are consistent with the measured hardness values, where the finer substructure at position K correlates with higher hardness, while the comparatively coarser features at position G are associated with a slight reduction in hardness.

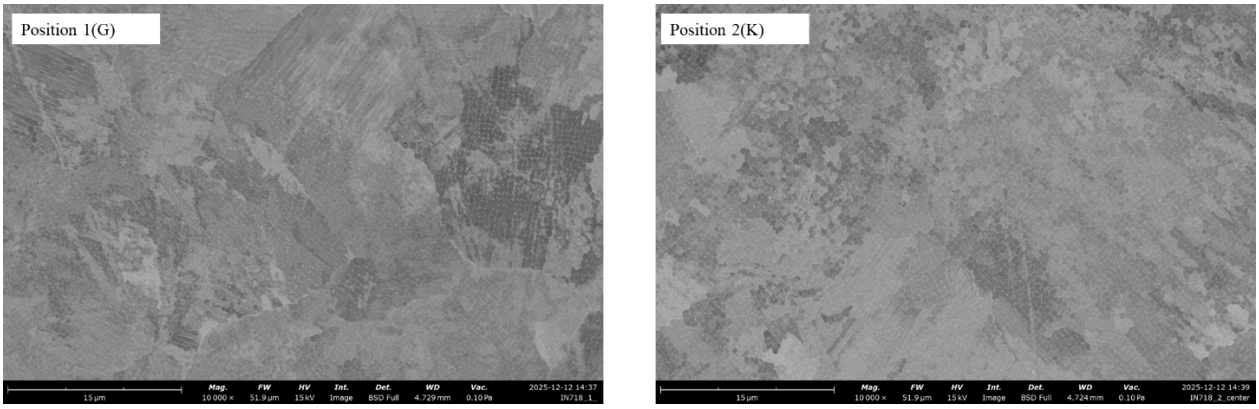

Fig. 4. SEM micrographs of the printed coupons at different build-plate temperature.

Hardness Results

The average hardness result of the printed samples is shown in Figure 5. Six hardness measurements were performed on each sample. The average hardness at position G was 274 HV0.5, whereas position K showed a higher average hardness of 280 HV0.5. The increase in hardness at position K can be attributed to the lower local build-plate temperature, which promotes higher cooling rates and results in a finer microstructural scale. In contrast, the elevated temperature at position G likely led to partial thermal softening or microstructural coarsening, reducing hardness.

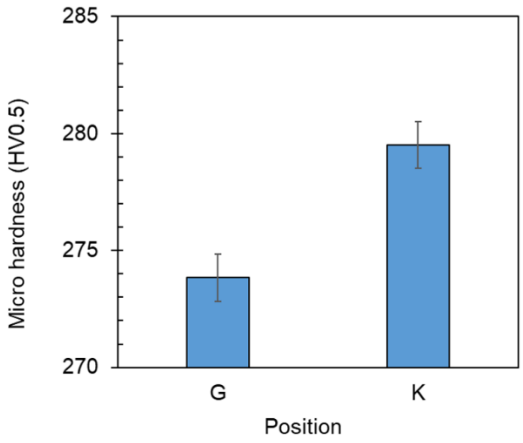

Fig. 5. Hardness results of samples printed at highest and lowest build-plate temperature.

Limitation

A limitation of the present study is that the spatial distribution of delivered laser energy across the build platform was not directly quantified. While build-plate temperature was experimentally mapped

and correlated with variations in microstructure and hardness, potential spatial variations in laser power density were not assessed within the scope of this work. Consequently, the individual contributions of laser-energy heterogeneity and build-plate temperature to the observed thermal and mechanical responses cannot be fully decoupled. Future investigations should therefore integrate spatially resolved laser-power monitoring together with thermal mapping to enable a more comprehensive evaluation of coupled process–thermal effects in LPBF.

Conclusion

This study investigated the influence of spatial variations in build-plate temperature on the porosity, microstructure, and hardness of Inconel 718 fabricated by laser powder bed fusion. Thermocouple-based measurements revealed pronounced non-uniformity in the build-plate temperature, with measured values ranging from approximately 101 °C to 120 °C despite a nominal set temperature of 180 °C. A clear radial temperature gradient was observed, with higher temperatures at the center of the build-plate and progressively lower temperatures toward the edges and corners, highlighting that the programmed build-plate temperature does not directly represent the local thermal boundary condition experienced during fabrication.

Volumetric porosity measured by micro-CT was essentially equal for the two sampled positions, however, the pore populations differed in architecture. The sample from the hotter location contained fewer but locally larger voids, whereas the colder location exhibited a higher number density of smaller pores distributed throughout the volume. This indicates that build-plate temperature influences defect-formation pathways even when net void volume is unchanged.

Microstructural characterization showed that samples fabricated at higher local build-plate temperatures exhibited a slightly coarser cellular–dendritic substructure, while samples printed at cooler locations displayed finer microstructural features consistent with higher cooling rates. These microstructural differences were reflected in the mechanical response, as samples produced at lower build-plate temperatures exhibited higher hardness values compared to those fabricated at warmer locations. The results demonstrate that spatial variations in build-plate temperature alone, even under nominally identical process parameters, can lead to measurable differences in microstructure and hardness within a single LPBF build.

Overall, the findings emphasize the importance of accounting for spatially varying thermal boundary conditions when evaluating process-structure-property relationships in LPBF. Local deviations in build-plate temperature can introduce unintended heterogeneity in material properties, which is particularly critical for components requiring high reliability and uniform performance. The results underscore the need for improved thermal management and localized process monitoring in LPBF systems to ensure consistent part quality across the build platform.

References

[1] T. DebRoy *u. a.*, „Additive manufacturing of metallic components – Process, structure and properties“, *Progress in Materials Science*, Bd. 92, S. 112–224, März 2018, doi: 10.1016/j.pmatsci.2017.10.001.

[2] M. McGregor, S. Patel, K. Zhang, A. Yu, M. Vlasea, und S. McLachlin, „A Manufacturability Evaluation of Complex Architectures by Laser Powder Bed Fusion Additive Manufacturing“, *Journal of Manufacturing Science and Engineering*, Bd. 146, Nr. 6, S. 061007, Juni 2024, doi: 10.1115/1.4065315.

[3] A. Ur Rehman, F. Pitir, und M. U. Salamci, „Laser Powder Bed Fusion (LPBF) of In718 and the Impact of Pre-Heating at 500 and 1000 °C: Operando Study“, *Materials*, Bd. 14, Nr. 21, S. 6683, Nov. 2021, doi: 10.3390/ma14216683.

[4] S. Chowdhury *u. a.*, „Laser powder bed fusion: a state-of-the-art review of the technology, materials, properties & defects, and numerical modelling“, *Journal of Materials Research and Technology*, Bd. 20, S. 2109–2172, Sep. 2022, doi: 10.1016/j.jmrt.2022.07.121.

[5] Q. Chen *u. a.*, „Elucidating the effect of preheating temperature on melt pool morphology variation in Inconel 718 laser powder bed fusion via simulation and experiment“, *Additive Manufacturing*, Bd. 37, S. 101642, Jan. 2021, doi: 10.1016/j.addma.2020.101642.

[6] J.-H. Park *u. a.*, „Effect of Preheating Temperature on Microstructural and Mechanical Properties of Inconel 718 Fabricated by Selective Laser Melting“, *Met. Mater. Int.*, Bd. 28, Nr. 11, S. 2836–2848, Nov. 2022, doi: 10.1007/s12540-022-01169-w.

[7] N. Baldi, A. Giorgetti, M. Palladino, I. Giovannetti, G. Arcidiacono, und P. Citti, „Study on the Effect of Preheating Temperatures on Melt Pool Stability in Inconel 718 Components Processed by Laser Powder Bed Fusion“, *Metals*, Bd. 13, Nr. 10, S. 1792, Okt. 2023, doi: 10.3390/met13101792.

[8] D. Bayoumy, T. Boll, A. S. Karapuzha, X. Wu, Y. Zhu, und A. Huang, „Effective Platform Heating for Laser Powder Bed Fusion of an Al-Mn-Sc-Based Alloy“, *Materials*, Bd. 16, Nr. 24, S. 7586, Dez. 2023, doi: 10.3390/ma16247586.

[9] E. Duong, L. Masseling, C. Knaak, P. Dionne, und M. Megahed, „Scan path resolved thermal modelling of LPBF“, *Additive Manufacturing Letters*, Bd. 3, S. 100047, Dez. 2022, doi: 10.1016/j.addlet.2022.100047.

[10] M. Tang, P. C. Pistorius, und J. L. Beuth, „Prediction of lack-of-fusion porosity for powder bed fusion“, *Additive Manufacturing*, Bd. 14, S. 39–48, März 2017, doi: 10.1016/j.addma.2016.12.001.

[11] J. S. Weaver, J. C. Heigel, und B. M. Lane, „Laser spot size and scaling laws for laser beam additive manufacturing“, *Journal of Manufacturing Processes*, Bd. 73, S. 26–39, Jan. 2022, doi: 10.1016/j.jmapro.2021.10.053.

[12] S. A. Khairallah, A. T. Anderson, A. Rubenchik, und W. E. King, „Laser powder-bed fusion additive manufacturing: Physics of complex melt flow and formation mechanisms of pores, spatter, and denudation zones“, *Acta Materialia*, Bd. 108, S. 36–45, Apr. 2016, doi: 10.1016/j.actamat.2016.02.014.